This article was downloaded by: [Renmin University of China]
On: 13 October 2013, At: 10:45
Publisher: Taylor & Francis
Informa Ltd Registered in England and Wales Registered Number: 1072954 Registered office: Mortimer House, 37-41 Mortimer Street, London W1T 3JH, UK

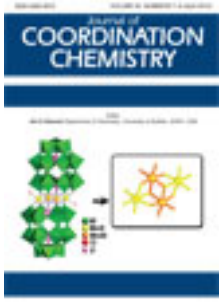

Journal of Coordination Chemistry
Publication details, including instructions for authors and subscription information:
http://www.tandfonline.com/loi/gcoo20

Synthesis and properties of zirconium(IV) and molybdate(II) morin complexes

Qadeer K. Panhwar [a b] & Shahabuddin Memon [b]

[a] Dr. M.A. Kazi Institute of Chemistry, University of Sindh , Jamshoro , Pakistan

[b] National Center of Excellence in Analytical Chemistry, University of Sindh , Jamshoro 76080 , Pakistan

Published online: 09 Mar 2012.

To cite this article: Qadeer K. Panhwar & Shahabuddin Memon (2012) Synthesis and properties of zirconium(IV) and molybdate(II) morin complexes, Journal of Coordination Chemistry, 65:7, 1130-1143, DOI: 10.1080/00958972.2012.668617

To link to this article: http://dx.doi.org/10.1080/00958972.2012.668617

PLEASE SCROLL DOWN FOR ARTICLE

Taylor & Francis makes every effort to ensure the accuracy of all the information (the "Content") contained in the publications on our platform. However, Taylor & Francis, our agents, and our licensors make no representations or warranties whatsoever as to the accuracy, completeness, or suitability for any purpose of the Content. Any opinions and views expressed in this publication are the opinions and views of the authors, and are not the views of or endorsed by Taylor & Francis. The accuracy of the Content should not be relied upon and should be independently verified with primary sources of information. Taylor and Francis shall not be liable for any losses, actions, claims, proceedings, demands, costs, expenses, damages, and other liabilities whatsoever or howsoever caused arising directly or indirectly in connection with, in relation to or arising out of the use of the Content.

This article may be used for research, teaching, and private study purposes. Any substantial or systematic reproduction, redistribution, reselling, loan, sub-licensing, systematic supply, or distribution in any form to anyone is expressly forbidden. Terms & Conditions of access and use can be found at http://www.tandfonline.com/page/terms-and-conditions

Journal of Coordination Chemistry
Vol. 65, No. 7, 10 April 2012, 1130–1143

Taylor & Francis
Taylor & Francis Group

Synthesis and properties of zirconium(IV) and molybdate(II) morin complexes

QADEER K. PANHWAR†‡ and SHAHABUDDIN MEMON*‡

†Dr. M.A. Kazi Institute of Chemistry, University of Sindh, Jamshoro, Pakistan
‡National Center of Excellence in Analytical Chemistry, University of Sindh, Jamshoro 76080, Pakistan

(*Received 30 October 2011; in final form 25 January 2012*)

Morin, an excellent chelating agent, has been used to form complex with a metal cation (Zr^{4+}) and a metal oxyanion (MoO_4^{2-}), isolating highly colored $[Zr(C_{15}H_9O_7)_2(NO_3)_2]\cdot 2H_2O$ (**1**) and $[MoO_3(C_{15}H_9O_7)_2]\cdot 3H_2O$ (**2**). The structures were elucidated using different techniques (i.e., electrical conductance, elemental, and thermal analyses) as well as a series of spectroscopic techniques (i.e., UV-Vis, IR, and ^1H NMR). The stoichiometry of the complexes is 1 : 2, confirmed by the molar ratio method. Zr^{4+} is useful for structural diagnosis of different flavonoids. The preferred site of complex formation of morin is the 3-hydroxy-4-keto system. Complex **2** is more stable than **1**. Fluorescence and cyclic voltammetry were studied. Antioxidative study affirmed that both **1** and **2** are efficient antioxidants relative to morin.

Keywords: Zirconium; Molybdenum; Morin; Antioxidant; Fluorescent

Downloaded by [Renmin University of China] at 10:45 13 October 2013

1. Introduction

Metal complexes of flavonoids have potential of being used as colorimetric reagents to determine the metal ions [1, 2]. Morin (figure 1), a light yellow bioactive pigment, is a main component of the flavonoid family, in wood of old fustic (*Chlorophora tinctoria*) or in yellow Brazil wood. It is mainly present in plants and plant-derived foods like coffee, tea, cereal grains, vegetables, and fruit and acts as a food preservative. Morin has a wide range of biological properties, i.e., anti-inflammatory, anticancer, antioxidant as well as cardiovascular protection [3–8].

Morin complexes many metal ions [9] as a chelate and is widely used as a probe for the detection of metal ions and some biomacromolecules, such as nucleic acid and protein [8]. It can selectively form highly colored and fluorescent complexes with metal ions [10]. With pK_a of 3.46, 3-OH is the most acidic proton in morin and studies have suggested that 3-OH has superior complexing power to 5-OH because 5-OH has strong hydrogen-bonding with oxygen of >C=O, facilitating a stable hexagonal

*Corresponding author. Email: shahabuddinmemon@yahoo.com

ISSN 0095-8972 print/ISSN 1029-0389 online © 2012 Taylor & Francis
http://dx.doi.org/10.1080/00958972.2012.668617

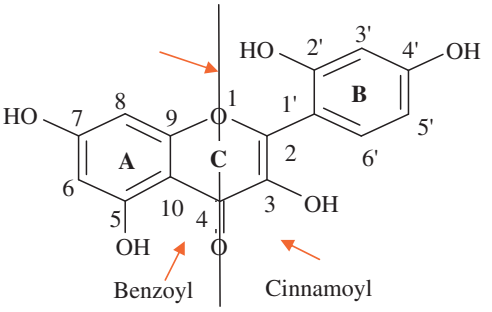

Figure 1. Chemical structure of morin (2′,3,4′,5,7-pentahydroxyflavone).

Downloaded by [Renmin University of China] at 10:45 13 October 2013

arrangement [4, 7]. At various conditions, morin association is different for Al 3 : 2 [10], Cu 1 : 1 [11], and Co, Ni, Zn 1 : 2, sometimes using different chelating sites by deprotonation of 2′-OH [12], 5-OH [7], and 3-OH [5].

Divalent metal chelates of morin are common, however, complexes of higher valent metal ions are rare [13]. The exocyclic group in combination with heterocycle containing oxygen produces substantial coordination power, dependent on nature of metal ion, pH of the medium, and reaction conditions [14].

Molybdenum is a micronutrient for animals, plants, and microorganisms, possessing tremendous biochemical value owing to its efficiency (a) for electron transfer due to easy interchange of its different oxidation numbers and (b) making strong bonds with oxygen, sulfur, and nitrogen donors. More than 50 enzymes of molybdenum are known, which catalyze important redox reactions. Recently, polyoxomolybdenum anions have been given attention due to their potential in solid state technology, catalysis, and medicine together with antivirus (HIV) and antitumor activity [15, 16]. Molybdenum performs an important role in different biological systems, but molybdenum salts have higher toxicity. Therefore we coordinate Mo^{6+} with biologically active morin having low toxicity [17]. Oxo-anions show marvelous antidiabetic character and play roles in inhibiting tyrosine phosphate enzyme *via* substituting phosphate at the active center, improving the insulin signaling. Oxo-anions like MoO_4^{2-} are not directly absorbed through the intestine hence delivery in the form of uncharged hydrophobic complex to be absorbed by intestine as well as transformed to molybdate in the blood stream is suggested. Complex supplied in that way must be stable under gastric and intestinal digestion conditions [18]. MoO_4^{2-} forms colored complexes with nucleophilic ligands in 1 : 1 and 1 : 2 metal-to-ligand ratios. From importance of morin and molybdenum, the synthesis and characterization of molybdenum(VI) complex is reported here to model oxomolybdenum enzymes [15, 16, 19].

Zirconium(IV) also forms complexes with biological value [20], with antitumor properties above cisplatin and functioning as efficient antifungal and antibacterial agents [21]. Zr^{4+} has been utilized here forming stable complexes with higher coordination numbers [20, 22, 23]. We report the synthesis, characterization, and the proposed structures for Zr^{4+} and Mo^{6+} complexes of morin.

Oxygen-reactive species, in particular free radicals, are involved in several diseases including cancer, atherosclerosis, and aging. Antioxidants have ability to scavenge excess free radicals; flavonoids are strong antioxidants. In this study, the relative

antioxidant activity of morin, **1**, and **2** have also been investigated. To our knowledge, no previous investigations have been done on radical scavenging effects of morin-based metal complexes [24, 25].

2. Experimental

2.1. *Materials*

All reagents and solvents were of analytical or chemically pure grade. Morin hydrate (2-(2,4-dihydroxyphenyl)-3,5,7-trihydroxy-4H-1-benzopyran-4-one) and (1,1-diphenyl-2-picrylhydrazyl) (DPPH$^{\bullet}$) were purchased from Sigma (St. Louis, MO, USA), zirconium nitrate and HPLC grade methanol from Fisher Scientific Ltd. (Leicestershire, UK), KBr from Aldrich Chemical Co. (Taufkirchen, Germany), and $LiClO_4$ as well as sodium molybdate were purchased from Fluka (Buchs, Switzerland). All the reagents were weighed with an accuracy of ± 0.0001 g.

Downloaded by [Renmin University of China] at 10:45 13 October 2013

2.2. *Physical measurements*

UV-Vis spectra were obtained by a Perkin-Elmer Lambda 35 UV-Vis double beam spectrophotometer using standard 1.00 cm quartz cells in methanol. ^{1}H NMR spectra were recorded on a Bruker 500 MHz spectrometer in DMSO using TMS as internal reference. FT-IR spectra were recorded from 4000 to 400 cm^{-1} on a Thermo Scientific Nicolet *i*S10 FT-IR instrument.

TG/DTA curves were obtained by using a Pyris Diamond TG/DTA (Perkin-Elmer Instrument, Technology by SII) under nitrogen at 20°C min^{-1} from ambient to 600°C. pH of the complexes was measured using an Inolab pH 720 WTW series pH meter. Electrolytic conductances of the complexes were measured by an Inolab cond 720 WTW series conductometer. Fluorescence spectra were recorded on a Shimadzu RF-5301PC spectrofluorophotometer using a quartz cell (1 cm × 1 cm cross-section). Cyclic voltammograms (CVs) of morin, **1**, and **2** were obtained at 25°C ± 1 from −0.5 to +1.4 V with scan rate 0.1 V s^{-1} using a conventional three electrode system with glassy carbon as working, platinum wire as auxiliary, and Ag/AgCl as reference electrode. $LiClO_4$ was used as supporting electrolyte.

2.3. *pH optimization for complexation*

The effect of pH on complexes was studied by adjusting the pH of metal solutions with 0.01 mol L^{-1} NaOH/HCl. The dependence of absorption spectra on pH was found maximum around pH 3.0–8.0 (i.e., 3.38 for **1** at 424 nm and 8.43 pH for **2** at 422 nm) and is less at pH 8.5–12 because these metals may be precipitated at higher pH [26–28]. The shape of absorption bands and position of maxima (Supplementary material) is unchanged in the pH range of 2–8 for both complexes. However, at higher pH values, absorption maxima either show a bathochromic or hypsochromic shift due to dissociation or formation of complexes with different stoichiometry [29, 30].

2.4. *Composition of the metal complexes (stoichiometry)*

Following Job's method (method of continuous variation), equimolar solutions (1×10^{-4} mol L^{-1} concentration) of morin as well as metal salts of zirconium nitrate and sodium molybdate were prepared in methanol. The solutions of morin and metal salts were mixed in appropriate ratios extending from 1 : 9 to 9 : 1 and the corresponding absorbances for morin and zirconium nitrate as well as morin and sodium molybdate were measured [11].

2.5. *Preparation of the complexes*

In a round bottom flask (50 mL), morin (0.302 g, 1 mmol) was dissolved (15 min) then zirconium nitrate (0.215 g, 0.5 mmol) or sodium molybdate (0.121 g, 0.5 mmol) was added. After 2 h of stirring, the solutions were filtered to eliminate undissolved/unreacted components; the precipitates were removed, washed with small aliquot of diethyl ether, and dried over silica gel in a vacuum desiccator. Finally, the complexes were dried in air; **1** was chocolate and **2** was maroon colored. The % yield of **1** and **2** were 75% and 61%, respectively. Elemental Anal. Found (%): C, 41.98; H, 2.63; N, 3.20. Anal. Calcd for $[Zr(C_{15}H_9O_7)_2(NO_3)_2]\cdot 2H_2O$ (%): C, 42.20; H, 2.58; N, 3.28. Similarly, the elemental Anal. Found (%): C, 45.33; H, 2.99. Anal. Calcd for $[MoO_3(C_{15}H_9O_7)_2]\cdot 3H_2O$ (%): C, 45.02; H, 3.02, respectively.

2.6. *The reactions of complex formation*

Reaction (1) for synthesis of **1** proceeds at very low pH:

$$Zr(NO_3)_4 + 2C_{15}H_{10}O_7 \rightleftharpoons \left[Zr(C_{15}H_9O_7)_2(NO_3)_2\right] + 2H^+ + 2NO_3^-, \quad (1)$$

$$MoO_4^{2-} + 2C_{15}H_9O_7H \rightleftharpoons \left[MoO_3(C_{15}H_9O_7)_2\right] + H_2O. \quad (2)$$

For synthesis of **2** (reaction 2), an opposite pH effect was observed. The first step involves the formation of molybdenum trioxide (reaction 3),

$$MoO_4^{2-} + 2H^+ \rightleftharpoons MoO_3 + H_2O, \quad (3)$$

which links to two ions of morin through the 3-hydroxyl and carbonyl groups. The pH increase of solution may be due to reactions 4 or 5 [31]:

$$2H^+ + MoO_4^{2-} \rightleftharpoons H_2MoO_4, \quad (4)$$

$$7H^+ + 6MoO_4^{2-} \rightleftharpoons HMo_6O_{21}^{5-} + 3H_2O. \quad (5)$$

2.7. *Physical properties of the complexes*

The analytical data as well as physical properties of **1** and **2** show that they are colored, non-hygroscopic, and thermally stable solids, suggesting a strong metal-to-ligand bond. The complexes are soluble in polar solvents, methanol, ethanol, DMF, and DMSO,

Downloaded by [Renmin University of China] at 10:45 13 October 2013

Table 1. Solubility information for **1** and **2**.

Complex	Soluble	Slightly soluble	Insoluble
1	MeOH, EtOH, DMF, DMSO	Acetone, H_2O	*n*-hexane, DCM, CCl_4, $CHCl_3$
2	MeOH, EtOH, DMF, DMSO	Acetone, H_2O	*n*-hexane, DCM, CCl_4, $CHCl_3$

slightly soluble in water and acetone [20] but insoluble in non-polar solvents (table 1). The molar conductances of 10^{-3} mol L^{-1} DMSO solutions were 24.5 and 23.7 μS cm^{-1} for **1** and **2**, respectively, corresponding to non-electrolytes [32]. Analytical and spectroscopic data show mononuclear complexes and two bidentate morin bound to one metal. Both the complexes are diamagnetic [16]. This assumption is in accord with elemental analysis, FT-IR, ^{1}H NMR, and UV-Vis spectroscopy [12].

Downloaded by [Renmin University of China] at 10:45 13 October 2013

2.8. *Antioxidant assay*

In the DPPH test, hydrogen atoms undergo exchange between antioxidant and DPPH radical (reaction 6), leading to reduction of DPPH radicals to hydrazine that is marked by the change of color from violet to yellow. The reaction was studied spectrophotometrically [33] with degree of decolorization taken as a measure of the reducing capacity of flavonoid.

$$DPPH^{\bullet} + AH \rightarrow DPPH - \mathrm{H} + \mathrm{A}^{\bullet}. \quad (6)$$

The samples were tested individually, where solutions contained 3.9 mL of DPPH (60 μmol L^{-1}) and 0.1 mL of different concentrations of morin extending from 1 to 20 μmol L^{-1} as an antioxidant standard and samples of **1** and **2**. The absorbances of the resulting solutions were measured at 515 nm against a blank sample containing only DPPH, the negative control. The decrease in absorbance at 515 nm, caused by the addition of flavonoid, was followed for 30 min and the scavenging activity (%) calculated by using equation (7),

$$\text{Scavenging activity (\%)} = \frac{(A_C - A_S)}{A_C} \times 100, \quad (7)$$

where A_C and A_S are the absorbance of control and sample, respectively [2, 34].

3. Results and discussion

3.1. *Synthesis and composition*

For the synthesis of **1** and **2**, Job's method of continuous variation was employed to determine the composition of chelate complexes. To find the exact ratio, the plots were extrapolated and the mole fraction of morin (X) was found at $X_L = 0.667$ (figure 2) according to their highest corresponding absorbance at 423 nm and 422 nm,

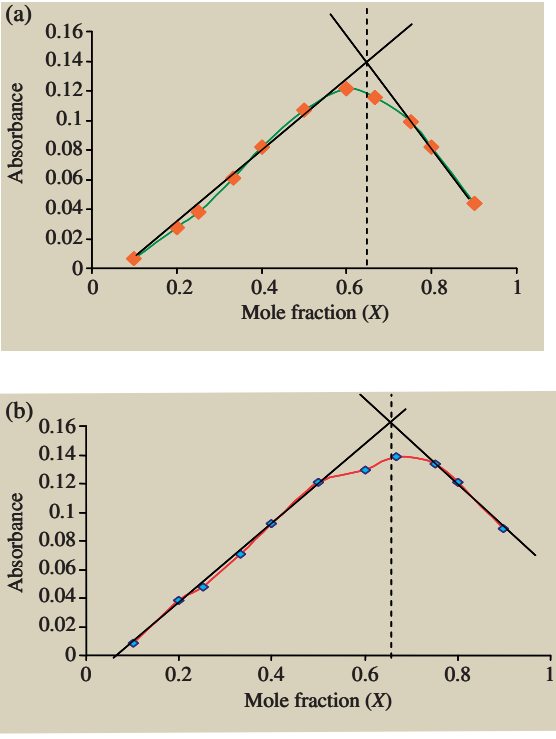

Figure 2. Job's plot for complexes of morin with (a) Zr^{4+} and (b) Mo^{6+} by mixing equimolar solutions of 1×10^{-4} mol L^{-1} each morin and metal salts.

(**1**) $[Zr(C_{15}H_9O_7)_2(NO_3)_2]\cdot 2H_2O$ (**2**) $[MoO_3(C_{15}H_9O_7)_2]\cdot 3H_2O$

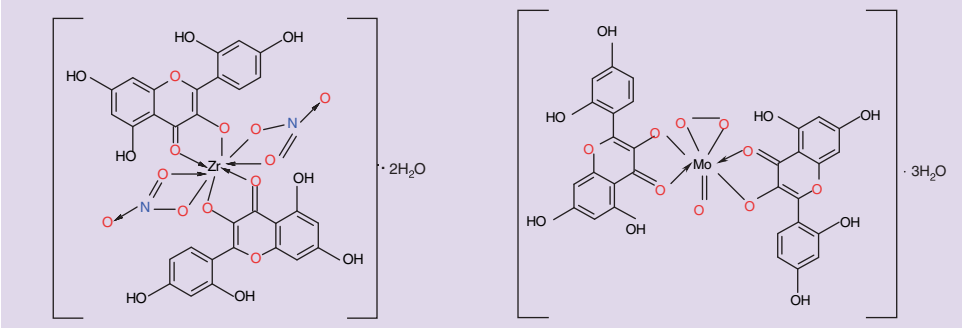

Scheme 1. Proposed coordination structures of **1** and **2**.

respectively. The stoichiometry of the corresponding complexes was thus 1 : 2 from the mole fraction value.

The stoichiometry of **1** was also determined applying the molar ratio method. The molar ratio plots show inflection at [Zr]/[morin] = 0.5, indicating the stoichiometric composition of 1 : 2 [10]. Possible structures for **1** and **2** are shown in scheme 1.

Downloaded by [Renmin University of China] at 10:45 13 October 2013

Table 2. UV-Vis data for morin, **1**, and **2**.

Compound	Morin	**1**	Δλ	**2**	Δλ
Band I	358 nm	423 nm	65 nm	422 nm	64 nm
Band II	253 nm	267 nm	14 nm	262 nm	09 nm

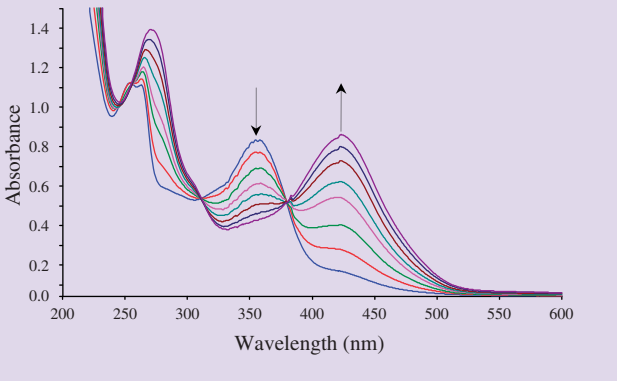

Figure 3. Electronic absorption spectra of morin (2.0×10^{-5} mol L^{-1}) in methanol during titration with Zr^{4+}. Concentration range: 0–28 μmol L^{-1}.

3.2. *Electronic spectra*

The UV-Vis spectrum of morin in methanol shows two major bands at 358 nm (band I) and 253 nm (band II). Band I is absorption of the cinnamoyl system, while band II is absorbance of the benzoyl system [11]. Spectral data for the absorbances of **1** and **2** are shown in table 2. Addition of Zr^{4+} and MoO_4^{2-} into morin solution causes red shift of the band at 358 nm to 423 nm for **1** and 422 nm for **2** [5]. Complex formation causing bathochromic shifts [11] of 65 and 64 nm to λ_{max} of morin [17] suggests formation of metal–oxygen bond in the cinnamoyl system (Supplementary material) [12].

3.3. *Spectrophotometric titrations*

For determination of stoichiometry of [Zr]/[morin] system, spectrophotometric (Supplementary material) titration was performed [35]. Due to low pK_a of the 3-hydroxychromone proton, the ligand was deprotonated. Figure 3 shows the two stage change of the absorption spectra of [Zr]/[morin] system [4, 9]. Following the spectral changes associated with the amount of Zr^{4+} added [35], decrease in the absorption band of morin at $\lambda_{max} = 358$ nm accompanied by the simultaneous increase in absorption at $\lambda_{max} = 423$ nm is ascribed to 1 : 2 for **1**. A unique isosbestic point (figure 4) was observed at 388 nm, indicative of the presence of a single complex formed [4]. In the molar ratio plot, curves of absorbance *versus* [Zr]/[morin] illustrated that the inflection at 0.5 is indicative of the 1 : 2 complex (ML_2) stoichiometry [35]. The new band at 423 nm corresponds to the formation of M-3-OH, forming a big extended π-bonding system

Downloaded by [Renmin University of China] at 10:45 13 October 2013

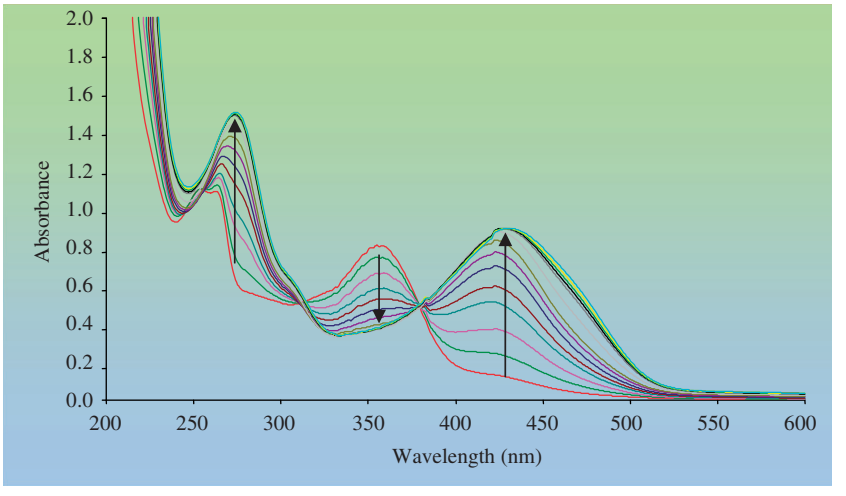

Figure 4. Spectrophotometric titration curves and spectra of morin in methanol (4×10^{-5} mol L^{-1}, 0): increasing concentrations of Zr^{4+} (from 4×10^{-6} mol L^{-1}, 0.1 to 8×10^{-5} mol L^{-1}).

with inclusion of C ring leading to further stabilization [36]. The electronic transition within morin changes from n–π^* to lower energy π–π^* favoring the development of a new band at higher wavelength [35].

The major difference between figures 3 and 4 is that at a low excess of Zr^{4+} the electronic spectra indicate formation of three isosbestic points due to the simultaneous presence of three species, i.e., metal (M), ligand (L), and complex (ML_2), while at large excess there is the formation of a single complex with only one isosbestic point.

A twofold excess of Zr^{4+} is necessary to obtain a full complexation of morin and excess of Zr^{4+} has no effect on the absorbance [6]. When morin reacts with excess of Zr^{4+}, a single complex formation reaction was observed as expected [4]. The zirconium and molybdate effect on the visible spectra (λ_{max}) of morin indicated that the behavior of [Mo]/[morin] system is not similar to the [Zr]/[morin] system because MoO_4^{2-} forms the complex at once while development of Zr^{4+} complex takes place slowly.

With excess Zr^{4+}, the 3-hydroxy-4-keto and the 5-hydroxy-4-keto systems cannot be discriminated, but with equimolar solutions a clear distinction is shown, because the 5-hydroxy-4-keto gives no bathochromic shift, whereas the 3-hydroxy-4-keto gives a value of 65 nm [37].

The low energy band at 423 nm may be assigned to an intense ligand-to-metal charge transfer transition produced through formation of a coordination bond between the unshared electron pair of C=O of morin and the d-orbital of metals (i.e., $O(\pi) \rightarrow M(d)$) due to promotion of electron from the highest occupied molecular orbital of ligand to lowest unoccupied molecular orbital of metal. The color of the complexes is due to charge transfer absorption tailing in from the ultraviolet [16, 17, 38].

3.4. *Vibrational spectra*

Structurally significant IR bands of morin and its complexes have been reported (Supplementary material) [1]. In **1** and **2**, almost all bands are shifted to lower frequency

Downloaded by [Renmin University of China] at 10:45 13 October 2013

Table 3. ^{1}H NMR data of morin, **1**, and **2**.

H	Morin	**1**	**2**
2′OH	9.40	8.297	6.204
4′OH	9.40	9.77	6.381
3OH	9.74	–	–
5OH	12.61	12.596	12.76
7OH	10.66	11.922	6.489

Downloaded by [Renmin University of China] at 10:45 13 October 2013

relative to morin [32]. The position of ν(C=O) is diagnostic for involvement of 4C=O in coordination, from 1666 cm^{-1} to 1621 cm^{-1} ($\Delta\nu = 45$ cm^{-1}) for **1** and 1660 cm^{-1} ($\Delta\nu = 6$ cm^{-1}) for **2** [7]. The band related to ν(C–O–C) at 1264 cm^{-1} is slightly shifted by complex formation in both cases, indicating the lack of interaction by ring oxygen [35].

In **1**, a broad band at 3194 cm^{-1} may be due to ν(O–H) indicating the existence of water, consistent with thermal analysis [12]; a sharp shoulder at 1544 cm^{-1} may be assigned to $\delta(H_2O)$. The medium band at 978–738 cm^{-1} is assigned to M–O mode in **1** [13], indicating that 3-OH group has been deprotonated with the formation of bond with metal [35]. The spectra show no absorption near 1352 cm^{-1}, where ionic nitrate absorbs, indicating the absence of ionic nitrate. Other bands at ~1501, ~1231, ~1011, and ~738 cm^{-1} correspond to ν_1, ν_4, ν_2, and ν_3, respectively, for bidentate nitrate. The separation between ν_1 and ν_4 bands indicates bidentate nitrate [20]. The position of Zr–O/Mo = O stretches are typical [35]. The band associated with 1596–1544 cm^{-1} is related to the formation of the chelate ring >C=O···M–O [7].

In the spectrum of **2**, a broad band at 3124 cm^{-1} due to ν(O–H) indicates water, supported by thermal analysis [17]. The metal peroxo gives rise to three characteristic IR modes, i.e., (O–O) stretching (ν_1) at 831–850 cm^{-1}, the symmetric (Mo–O) stretching (ν_2) at 650–697 cm^{-1}, and asymmetric (Mo–O) stretching (ν_3) at 730–746 cm^{-1} [15]. Complex **2** shows distorted octahedral structure with *cis*-oxygen atoms having strong bands at 968–981 cm^{-1} assigned to stretch of terminal Mo=O [38]. A new weak peak at 550 cm^{-1} is assigned to ν(Mo–O) [16], consistent with coordination *via* carbonyl oxygen [19].

3.5. *^{1}H NMR studies*

Complexation occurs with loss of 3-hydroxyl proton and leads to destruction of hydrogen bonds. Assignments for protons of hydroxyl of morin are given by literature data. The relative chemical shift values for protons of morin and **1** and **2** are presented in table 3. Four signals of hydroxyl groups are visible in spectra of complexes. All the ring protons undergo the shifts in their resonances, probably due to fixation of ring B caused by coordination [12].

3.6. *Thermal analysis*

Thermal decomposition was carried out under nitrogen at 30–600°C. Complex **1** undergoes decomposition in three main stages of weight loss (Supplementary material).

Table 4. Stability constants of **1** and **2** at various temperatures.

System	Temperature (K)	ln K
1	298	10.52
	303	10.38
	308	10.18
	313	10.04
2	298	12.50
	303	12.36
	308	12.29
	313	12.25

Downloaded by [Renmin University of China] at 10:45 13 October 2013

First of 9.6% pertains to endothermic dehydration at 30–110°C. The second weight loss of 12.4% is slow and continuous weight loss of nitrates strongly bonded with zirconium. Its decomposition starts at 110°C as T_i, reaches T_{max} at 240°C, and finally completes at 360°C as T_f. Final weight loss of 42% is from morin at 360–530°C as a moderately broad exothermic peak.

Weight loss curve of **2** shows continuous degradation. Removal of water as a small broad endothermic peak on the DTA curve at 96°C has corresponding weight loss of 16.4%, while the second mass loss stage was from decomposition of peroxo from 96°C to 165°C with 3.7% mass loss. Finally, degradation of morin takes place to 530°C as a big exothermic peak for 77.6% weight loss [12, 39].

3.7. *Stability constants and thermodynamic parameters*

The stability constants (table 4) and thermodynamic parameters (ΔG, ΔH, and ΔS) (table 5) of **1** and **2** were studied at 25°C, 30°C, 35°C, and 40°C by spectrophotometry [40]. Morin is bidentate and both complexes show stoichiometry of 1 : 2. By using measured absorbance, since it pertains only to ML_2, the molar absorption coefficients (ε) were determined from Beer's law ($A = \epsilon bc$). Equation (8) can be written for the stability constants of complexes.

$$K = \frac{[ML2]}{[M][L]^2} = \frac{[ML2]}{(CM - [ML2])(CL - 2[ML2])^2}. \tag{8}$$

In equation (8), if A/ε is substituted for [ML_2], it becomes:

$$K = \frac{A/\varepsilon}{(C_M - A/\varepsilon)(C_L - 2A/\varepsilon)^2}, \tag{9}$$

where A is the measured absorbance and ε is the molar absorption coefficient. The K can be calculated from equation (9).

For each temperature, graphs of ln K *versus* $1/T$ were plotted (figure 5). A straight line was obtained from which ΔG, ΔH, and ΔS for the complexes were calculated from slope ($-\Delta H/R$) and the intercept ($\Delta S/R$) of the plot. The average values of ln K of metal complexes were inversely proportional to the temperature [40, 41].

When the values of all the parameters were compared for both the complexes, it was found that **1** revealed larger negative enthalpy value due to significant change in total

Table 5. Thermodynamic parameters of **1** and **2**.

System	Temperature (K)	$-\Delta G$ (kJ mol^{-1})	$-\Delta H$ (kJ mol^{-1})	$+\Delta S$ (J mol^{-1} K^{-1})
1	298	34.82	25.02	0.00354
	303	26.15		
	308	26.06		
	313	26.13		
2	298	30.96	12.90	0.06
	303	31.13		
	308	31.47		
	313	31.87		

Downloaded by [Renmin University of China] at 10:45 13 October 2013

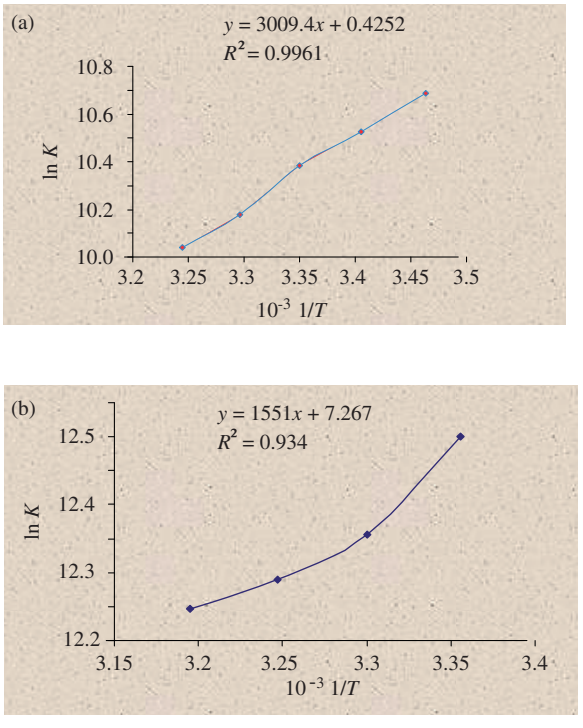

Figure 5. Plots of $\ln K$ *vs.* $1/T$ for the determination of thermodynamic parameters depicted for (a) **1** and (b) **2**.

internal energy on formation. Complex **2** showed greater negative ΔG [42]. ΔG and ΔH show high thermal stability of both complexes and reveal spontaneous and enthalpy-stabilized process, but mainly entropy driven. The large ΔS values suggest strong desolvation of the ligands, resulting in weak solvent–ligand interactions [42, 43].

3.8. *Structure of the complexes*

The structures of **1** and **2** have been deduced from UV-Vis, IR, and NMR spectroscopies [7]. Morin can bind through C(3)–OH and C(4)=O or *via* C(5)–OH

Table 6. Fluorescence data of morin, **1**, and **2**.

Compound/complex	Emission wavelength (nm)	Relative fluorescence intensity
Morin	497	57.5
1	488	75.9
2	490	63.7

and C(4)=O. Highly stable five-member chelate complexes are formed *via* binding through C(3)–O and C(4)=O, as opposed to six-element chelates of less stability [32].

On the basis of spectral and physicochemical data, structures of **1** and **2** are shown in scheme 1 [16].

Anions like MoO_4^{2-} form highly stable complexes since the metal-to-ligand interactions are partially electrostatic [44,45].

3.9. *Fluorescence spectroscopy*

Table 6 lists the fluorescence data for morin, **1**, and **2**; "Supplementary material" illustrates their emission spectra. Strong fluorescence was emitted at 497 nm by morin, while **1** and **2** have emission wavelengths of 490 and 488 nm, respectively [46]. The emissions by complexes are attributable to the fluorescence from intraligand emission excited states [47] with enhanced fluorescence intensity. The coordination of small highly charged Zr^{4+} and Mo^{6+} increase the fluorescence intensity by increasing rigidity of the ligand structure and reducing non-radiative energy dissipation. Complex **1** has higher intensity of fluorescence than **2**.

3.10. *Cyclic voltammetry*

From the CVs of morin, **1**, and **2**, the complexes exhibit well-defined oxidation peaks and virtually no reverse reduction peaks corresponding to irreversible reactions. The electrochemical processes involve only one electron transfer and one-step mechanism for oxidation in each compound. Morin presents one oxidation at +0.658 mV characteristic to 3-OH oxidation. The electrochemical data imply that coordination of metal facilitates oxidation by destabilizing the structure of flavonoid [47, 48].

3.11. *Antioxidant activity*

Flavonoids have remarkable antioxidative assets and antioxidant activity is affected by metal chelation [49]. Figure 6 shows the outcome of DPPH free radical scavenging. Morin, **1**, and **2** scavenge DPPH free radical with antioxidant power of **1** and **2** higher than morin [25].

4. Conclusion

Morin forms 1 : 2 complexes with Zr^{4+} and MoO_4^{2-} at pH of 3–8. Spectroscopic studies confirm complex formation; UV-Vis showed bathochromic shifts, IR revealed

Downloaded by [Renmin University of China] at 10:45 13 October 2013

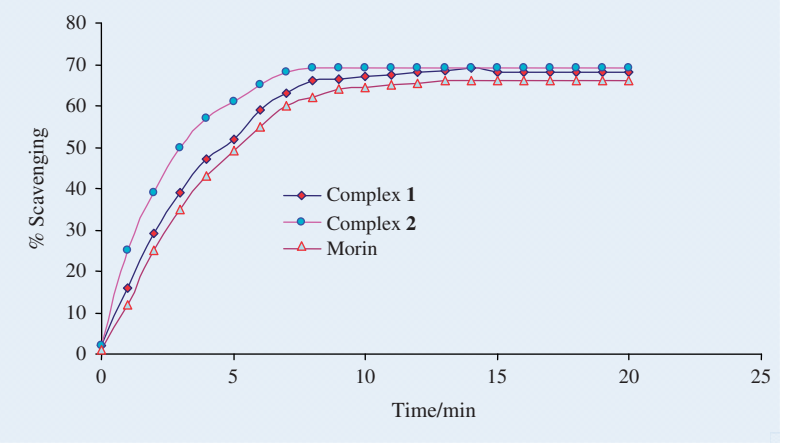

Figure 6. Scavenging activity of morin, **1**, and **2** to DPPH radical.

formation of M–O bonds and NMR proved replacement of 3-hydroxy proton by metals. Stability constants demonstrate formation of stable complexes. Fluorescence studies illustrate that morin, **1**, and **2** are fluorescent. Cyclic voltammetric studies show reactions with one electron transfer through a one-step reaction mechanism. Morin is a potent antioxidant and its complexes are stronger antioxidants than it.

Downloaded by [Renmin University of China] at 10:45 13 October 2013

Acknowledgments

This research work was supported by the National Centre of Excellence in Analytical Chemistry, University of Sindh, Jamshoro, Pakistan. The authors thank and gratefully acknowledge for this assistance and express their appreciations on the provision of necessary facilities.

References

[1] S.R. Yaul, A.R. Yaul, G.B. Pethe, A.S. Aswar. *Am-Euras. J. Sci. Res.*, **4**, 229 (2009).
[2] Q.K. Panhwar, S. Memon. *J. Coord. Chem.*, **64**, 2117 (2011).
[3] T.W. Wu, K.P. Fung, L.H. Zeng, J. Wu, A. Hempel, A.A. Grey, N. Camerman. *Biochem. Pharm.*, **49**, 537 (1995).
[4] P. Ryan, M.J. Hynes. *J. Inorg. Biochem.*, **102**, 127 (2008).
[5] Q.-L. Tian, S.-H. Liao, P. Lu, L.-J. Liu. *Chin. J. Chem.*, **24**, 1388 (2006).
[6] G. Zhang, J. Guo, J. Pan, X. Chen, J. Wang. *J. Mol. Struct.*, **923**, 114 (2009).
[7] E. Woznicka, M. Kopacz, M. Umbreit, J. Klos. *J. Inorg. Biochem.*, **101**, 774 (2007).
[8] P. Xiao, Q. Zhou, F. Xiao, F. Zhao, B. Zeng. *Int. J. Electrochem. Sci.*, **1**, 228 (2006).
[9] A.C. Gutierrez, M.H. Gehlen. *Spectrochim. Acta, Part A*, **58**, 83 (2002).
[10] C. Septhum, V. Rattanaphani, S. Rattanaphani. *Suranaree J. Sci. Technol.*, **14**, 91 (2007).
[11] Q.K. Panhwar, S. Memon, M.I. Bhanger. *J. Mol. Struct.*, **967**, 47 (2010).
[12] Z. Qi, W. Liufang, L. Xiang. *Transition Met. Chem.*, **21**, 23 (1996).
[13] P.S. Deshmukh, A.R. Yaul, J.N. Bhojane, A.S. Aswar. *World Appl. Sci. J.*, **9**, 1301 (2010).

[14] S. Sinha, A.K. Srivastava, C.M. Tripathi, O.P. Pandey, S.K. Sengupta. *Bioinorg. Chem. Appl.*, **2007**, 87918 (2007).
[15] R.C. Maurya, S. Sahu, P. Bohre. *Ind. J. Chem.*, **47A**, 1333 (2008).
[16] M. Nair, L.H. Nair, D. Thankamani. *J. Serb. Chem. Soc.*, **76**, 221 (2011).
[17] R.Kh. Yuldashev, Kh.M. Makhkamov, Kh.T. Sharipov, Kh.U. Aliev. *Chem. Nat. Prod.*, **35**, 420 (1999).
[18] S.J. Lord, N.A. Epstein, R.L. Paddock, C.M. Vogels, T.L. Hennigar, M.J. Zaworotko, N.J. Taylor, W.R. Driedzic, T.L. Broderick, S.A. Westcott. *Can. J. Chem.*, **77**, 1249 (1999).
[19] A.O. Aliyu. *Curr. Res. Chem.*, **2**, 35 (2010).
[20] Y.S. Malghe, R.C. Prabhu, R.W. Raut. *Drug Res.*, **66**, 45 (2009).
[21] R. Kaushal, R.K. Kaushal. Selective antibacterial activity of some novel zirconium complexe(s). In *XVIII International Conference on Bioencapsulation*, Porto, Portugal, 1–2 October (2010).
[22] R.D. Madan. *Satya Prakash's Modern Inorganic Chemistry*, S. Chand & Company Ltd., Ram Nagar, New Delhi, India (2006).
[23] F.A. Cotton, G. Wilkinson. *Basic Inorganic Chemistry*, Wiley & Sons, New York, USA (1921).
[24] A. Braca, C. Sortino, M. Politi, I. Morelli, J. Mendez. *J. Ethnopharma.*, **79**, 379 (2002).
[25] W. Chen, S. Sun, W. Cao, Y. Liang, J. Song. *J. Mol. Struct.*, **918**, 194 (2009).
[26] B. Dev, B.D. Jain. *J. Less-Common Metals*, **4**, 286 (1962).
[27] H. Filik, M. Dogutan, E. Tutem, R. Apak. *Anal. Sci.*, **18**, 955 (2002).
[28] M. Katyal, R.P. Singh. *Proc. Math. Sci.*, **56**, 125 (1962).
[29] V.S. Kuntic, D.L. Malesev. *J. Agric. Food Chem.*, **46**, 5139 (1998).
[30] D. Malesev, V. Kuntic. *J. Serb. Chem. Soc.*, **72**, 921 (2007).
[31] D. Malesev, Z. Radovic, M. Jelikic-Stankov. *Monatsh. Chem.*, **122**, 429 (1991).
[32] M. Kopacz, E. Woznicka. *Polish J. Chem.*, **78**, 521 (2004).
[33] L. Stanojević, M. Stanković, V. Nicolić, L. Nicolić, D. Ristić, J. Čanadanovic-Brunet, V. Tumbas. *Sensors*, **9**, 5702 (2009).
[34] M.M. Silva, M.R. Santos, G. Caroco, R. Rocha, G. Justino, L. Mira. *Free Rad. Res.*, **36**, 1219 (2002).
[35] E.G. Ferrer, M.V. Salinas, M.J. Correa, L. Naso, D.A. Barrio, S.B. Etcheverry, L. Lezama, T. Rojo, P.A.M. Williams. *J. Biol. Inorg. Chem.*, **11**, 791 (2006).
[36] A.A. Ensafi, R. Hajian, S. Ebrahimi. *J. Braz. Chem. Soc.*, **20**, 266 (2009).
[37] B.S. Sekhon, G.P. Kaushal, I.S. Bhatia. *Mikrochim. Acta*, **80**, 421 (1983).
[38] D.A. Chowdhury, M.N. Uddin, A.K.M.L. Rahman. *Chiang Mai. J. Sci.*, **33**, 357 (2006).
[39] J. Pusz, B. Nitka, S. Kopacz, Y.I. Korenman. *Russ. J. Gen. Chem.*, **73**, 634 (2003).
[40] S.N. Chadar, F. Khan, S. Sharma. *CHEMIJA*, **19**, 1 (2008).
[41] E.G. Akgemci, T. Atalay. *Turk. J. Chem.*, **24**, 89 (2000).
[42] K. Ali, N. Fatima, Z.T. Maqsood. *Scientia Iranica*, **21**, 311 (2005).
[43] O.E. Offiong. *Transition Met. Chem.*, **23**, 553 (1998).
[44] M. Gruzal, E. Budzisz. *Coord. Chem. Rev.*, **253**, 2588 (2011).
[45] K. Zare, N. Osouledini, M. Monajjemi. *J. Sci. I. A. U.*, **16**, 24 (2006).
[46] W.-S. Liao, F.-Y. Wu, Y.-M. Wu, X.-J. Wang. *Microchim. Acta*, **162**, 147 (2008).
[47] R.F.V. de Souza, W.F. De Giovani. *Spectrochim. Acta, Part A*, **61**, 1985 (2005).
[48] A. Pekal, M. Biesaga, K. Pyrzynska. *Biometals*, **24**, 41 (2011).
[49] N. Binbuga, W.P. Henry, T.P. Schultz. *Polyhedron*, **26**, 6 (2007).

Downloaded by [Renmin University of China] at 10:45 13 October 2013